Oxidative Stress-Responsive Intracellular Regulation Specific for the Angiostatic Form of Human Tryptophanyl-tRNA Synthetase†

Keisuke Wakasugi,*,‡,§ Tomomi Nakano,§ and Isao Morishima*,‡

Department of Molecular Engineering, Graduate School of Engineering, Kyoto University, Kyoto 615-8510, Japan, and PRESTO, Japan Science and Technology Agency, 4-1-8 Honcho Kawaguchi, Saitama 332-0012, Japan

Received August 6, 2004; Revised Manuscript Received October 19, 2004

ABSTRACT: Tryptophanyl-tRNA synthetase (TrpRS) exists in two forms in human cells, i.e., a major form which represents the full-length protein and a truncated form (mini TrpRS) in which an NH_2-terminal extension is deleted because of alternative splicing of its pre-mRNA. Mini TrpRS can act as an angiostatic factor, while full-length TrpRS is inactive. We herein show that an oxidized form of human glyceraldehyde-3-phosphate dehydrogenase (GapDH) interacts with both full-length and mini TrpRSs and specifically stimulates the aminoacylation potential of mini, but not full-length, TrpRS. In contrast, reduced GapDH did not bind to TrpRSs and did not influence their aminoacylation activity. Mutagenesis experiments clarified that the NH_2-terminal Rossmann fold region of GapDH is crucial for its interaction with mini TrpRS as well as tRNA and for the regulation of its aminoacylation potential and suggested that monomeric GapDH can bind to mini TrpRS and stimulate its aminoacylation activity. These results suggest that the angiostatic human mini, but not the full-length, TrpRS may play an important role in the intracellular regulation of protein synthesis under conditions of oxidative stress.

Aminoacyl-tRNA synthetases are key enzymes in protein biosynthesis that catalyze aminoacylation of their cognate tRNAs. Mammalian tryptophanyl-tRNA synthetases (TrpRSs)[1] have an appended domain at their NH_2 termini that is absent from lower eukaryotic and prokaryotic TrpRSs (*1*−*3*). The NH_2-terminal extensions of mammalian TrpRSs share homologous amino acid sequences with the linker peptide connecting the two catalytic domains of bifunctional glutamyl-prolyl-tRNA synthetase, the NH_2-terminal domains of glycyl- and histidyl-tRNA synthetases, and the COOH-terminal domain of methionyl-tRNA synthetase (*3*−*7*). These conserved domains have helix−turn−helix architectures and are essential for tRNA binding and for the enzymatic activities of aminoacyl-tRNA synthetases (*4*−*7*). Recently, the tertiary structures of TrpRSs have been determined (*8*−*10*); analysis of full-length TrpRS clarified that its NH_2-terminally appended domain forms a helix−turn−helix structure (*8*, *11*).

In human cells, TrpRS exists in two forms, i.e., a major form that is the full-length protein (amino acids 1−471) and a truncated form (mini TrpRS) (amino acids 48−471) in which most of the extra NH_2-terminal extension (amino acids 1−47) is deleted because of alternative splicing of the pre-mRNA (*2*, *12*−*14*). The expression level of both human full-length and mini TrpRSs is highly upregulated in human cells by the addition of interferon-γ (IFN) (*14*−*16*). Mini TrpRS was shown to have angiostatic activity, while the full-length enzyme was found to be inactive (*17*). The NH_2-terminal domain, which can be deleted by alternative splicing, may regulate the angiostatic activity of TrpRS by revealing a binding site that is necessary for angiostasis that is inaccessible in full-length TrpRS (*8*, *11*).

It has been shown that bovine TrpRS can form a complex with glyceraldehyde-3-phosphate dehydrogenase (GapDH) (*18*). GapDH is a key glycolytic enzyme, utilizing NAD^+ as a coenzyme for the oxidative phosphorylation of glyceraldehyde 3-phosphate to 1,3-diphosphoglycerate when assembled as a tetramer of identical 36 kDa subunits. It has been reported that GapDH is a target for oxidative stress (*19*) and that reactive and catalytically essential cysteine (Cys) in GapDH can be oxidized to its sulfenate derivative by hydrogen peroxide generated under oxidative stress conditions (*20*, *21*). The same Cys that is involved in that reaction is a target for nitric oxide-induced S-nitrosylation or S-glutathionylation in GapDH (*22*, *23*). S-Thiolation of this Cys in GapDH was induced by a phagocytosis-associated respiratory burst in blood monocytes (*24*). It should also be noted that GapDH also binds to tRNAs, and that this binding is enhanced by the oxidation of GapDH (*25*, *26*).

† This work was supported in part by Grants-in-Aid 13780532 and 15770085 for Young Scientists (B) (to K.W.), Grant-in-Aid 12215077 for Scientific Research on Priority Areas (to K.W.), and Grant-in-Aid 12002008 for Specially Promoted Research (to I.M.) from the Ministry of Education, Culture, Sports, Science and Technology of Japan.

* To whom correspondence should be addressed: Department of Molecular Engineering, Graduate School of Engineering, Kyoto University, Kyoto 615-8510, Japan. Telephone: 81-75-383-2537. Fax: 81-75-383-2541. E-mail: kei@wakasugi.mbox.media.kyoto-u.ac.jp.

‡ Kyoto University.

§ Japan Science and Technology Agency.

[1] Abbreviations: TrpRS, tryptophanyl-tRNA synthetase; IFN, interferon; GapDH, glyceraldehyde-3-phosphate dehydrogenase; SPR, surface plasmon resonance; IPTG, isopropyl β-D-thiogalactopyranoside; BSA, bovine serum albumin; RU, resonance units; Ngb, neuroglobin; MHC, major histocompatibility complex.

10.1021/bi048313k CCC: $30.25
Published on Web 12/02/2004

In this study, we determined whether the oxidized or reduced form of human GapDH could bind to full-length or mini TrpRS using surface plasmon resonance (SPR) measurements and examined whether its interaction with GapDH altered the aminoacylation of TrpRS. Structural and functional analyses, using a chimeric protein, were also performed. Finally, the biological significance of the interaction between human GapDH and TrpRS was discussed.

EXPERIMENTAL PROCEDURES

Samples. GapDH from human erythrocyte (Sigma, St. Louis, MO) was used. Oxidized and reduced forms of human GapDH were prepared by incubating it with 70 μM H_2O_2 and 2 mM β-mercaptoethanol for 30 min, respectively. Brewer's yeast tRNA was purchased from Roche Diagnostics (Basel, Switzerland). Human $tRNA^{Trp}$ was synthesized as synthetic oligonucleotides and was purified by polyacrylamide gel electrophoresis (Dharmacon Research, Lafayette, CO).

Preparation of Full-Length and Mini TrpRSs, Full-Length and Truncated GapDHs, and Wild-Type Myoglobin (Mb). cDNA fragments of human TrpRS, GapDH, and Mb were amplified by PCR using human universal Quick-clone cDNA (Clontech, Palo Alto, CA). Human full-length TrpRS (amino acids 1−471), mini TrpRS (amino acids 48−471) (*17*), full-length GapDH (amino acids 1−335), truncated GapDH (amino acids 1−150), and full-length Mb genes, including a COOH-terminal tag of six histidine residues (six-His tag), were cloned into plasmid PET20b (Novagen, Madison, WI), and the resulting vectors were sequenced with an ABI 3100 Genetic Analyzer (Applied Biosystems, Foster City, CA). Cys^{110} of human Mb was replaced with Ala to prevent difficulties in protein purification (*27*). In this study, we denote this mutant of human Mb as the "wild type". Proteins were overexpressed in *Escherichia coli* strain BL21(DE3) (Novagen) by induction with isopropyl β-D-thiogalactopyranoside (IPTG) for 4 h. Using the procedures described by Novagen, the proteins were purified on a nickel affinity column (His·Bind resin, Novagen) from the supernatant of lysed cells. After purification, TrpRSs were incubated with phosphate-buffered saline containing 1 μM $ZnSO_4$, and then free Zn^{2+} was removed (*28*). Protein concentrations were determined by the Bradford assay using bovine serum albumin (BSA) (Sigma) as the standard (Bio-Rad, Hercules, CA).

Preparation of Modules(GapDH)-Fused Mb. PCR fragments of human truncated GapDH (amino acids 1−148) and human wild-type Mb were cloned into prokaryotic expression vector PET20b to produce modules(GapDH)-fused Mb, in which the NH_2-terminal Rossmann fold modules of GapDH (amino acids 1−148) were fused to the NH_2 terminus of wild-type Mb, with the six-His tag. Its DNA sequence was confirmed by the dye deoxy terminator method using an ABI 3100 genetic analyzer (Applied Biosystems).

Modules(GapDH)-fused Mb was overexpressed in *E. coli* BL21(DE3) by induction with IPTG. The cell pellet, resuspended in buffer A [8 M urea and 20 mM Tris-HCl (pH 7.9)], was disrupted by freezing and thawing and was sonicated with ASTRASON XL2020 (Misonix, Farmingdale, NY). The supernatant was then applied to a Sepharose CL-6B cation-exchange column (Amersham Biosciences, Piscataway, NJ) equilibrated with buffer A and was eluted with a linear NaCl gradient from 0 to 1 M. The fraction containing the fusion protein was applied to a His·Bind resin (Novagen) equilibrated with buffer B [8 M urea, 20 mM Tris-HCl, and 500 mM NaCl (pH 7.9)] containing 5 mM imidazole. The column was washed with buffer B containing 60 mM imidazole, and was eluted with buffer B containing 1 M imidazole. The fraction including the fusion protein was diluted 16-fold with buffer C [20 mM borate-NaOH, 50 mM NaCl, and 1 mM EDTA (pH 9.3)] and was then mixed with 1.2 equiv of hemin. The solution was left for 4 h at 4 °C and was applied to a Sephadex G-25 (Amersham Biosciences) column that had been equilibrated with buffer D [20 mM potassium phosphate, 50 mM KCl, and 1 mM EDTA (pH 7.4)]. To measure the molecular sizes of proteins, gel filtration chromatography was performed by using a Superdex 200 HR 10/30 column for the FPLC system (Amersham Biosciences).

Since ferrous oxygen-bound modules(GapDH)-fused Mb is unstable and is converted into the ferric form through autoxidation, ferrous carbon monoxide (CO)-bound globins were used for the SPR measurements and aminoacylation assays. Ferrous CO-bound forms of modules(GapDH)-fused Mb and wild-type Mb were generated by adding sodium dithionite and CO gas to the ferric forms followed by gel filtration.

SPR Experiments. SPR measurements were performed on a BIAcore X instrument (Biacore, Uppsala, Sweden). Human full-length and mini TrpRSs were immobilized on the surface of a CM5 sensor chip using an amine coupling kit (Biacore) according to the instructions of the manufacturer. Briefly, carboxymethylated dextran in the CM5 sensor chip was activated by mixing equal volumes of 400 mM *N*-ethyl-*N*′-[3-(dimethylamino)propyl]carbodiimide in water and 100 mM hydrochloride and *N*-hydroxysuccinimide in water, and injecting the mixture at 10 μL/min for 7 min. A solution of 5 μg/mL TrpRS dissolved in 10 mM acetate buffer (pH 4.5) was then injected over the activated surface of the sensor chip for 7 min at a flow rate of 10 μL/min. Unreacted sites on the sensor chip were masked by injecting 1 M ethanolamine (pH 8.5) for 7 min. After the immobilization process, nonspecifically bound protein was removed by washing with running buffer [10 mM Hepes, 150 mM NaCl, and 0.005% Tween 20 (pH 7.4)] until the value of resonance units (RU) became nearly constant.

All binding experiments were performed at 25.0 °C at a flow rate of 5 μL/min. GapDH in the running buffer was injected for 2 min. Running buffer alone was then applied over the next 4 min. The BIAcore response is expressed in relative RU, i.e., the difference in response between the flow cell with the immobilized protein and the control flow channel; 1000 RU corresponds to 1 ng/mm^2 of bound ligand. After each binding cycle, the sensor chip was regenerated with 5 μL of 0.05% SDS in the running buffer and was washed with the running buffer for 5−10 min prior to the next injection. Experimental curves (sensorgrams) were analyzed with the BIAevaluation 3.1 software package using the A + B ⇔ AB model to estimate association and dissociation rate constants k_a and k_d.

Aminoacylation Assays. Aminoacylation activity was assayed at ambient temperature (∼20 °C) in buffer containing

the following: 150 mM Tris-HCl (pH 7.5), 150 mM KCl, 10 mM $MgCl_2$, 4 mM ATP, 33 μM tryptophan (Trp), and 5 μM [^{3}H]Trp (Amersham Biosciences). The reactions were initiated by adding TrpRS samples (50 nM) to the buffer that included brewer's yeast tRNA (5−500 μM) or human $tRNA^{Trp}$ (5 μM). Reaction samples were taken at 1 min intervals and spotted onto a Whatman 3MM paper filters. After 1 min, the filter disks were added to cold 5% trichloroacetic acid that included 2 mM Trp. The filters were washed three times with cold 5% trichloroacetic acid and 2 mM Trp, washed twice with ethanol, and washed once with ether, after which they were subjected to scintillation counting. Prior to the assays, the tRNA substrate was heated at 70 °C for 2 min and reannealed at ambient temperature for 30 min.

RESULTS

SPR Detection of Human GapDH Binding to Human TrpRS. SPR is a powerful tool for real time measurement of direct protein−protein interactions without labels. We covalently coupled human full-length or mini TrpRS to a BIAcore sensor chip and characterized the interaction between TrpRS and GapDH. Representative sensorgrams are shown in panels A and B of Figure 1, which demonstrate that the resonance responses reflecting GapDH−full-length and −mini TrpRS interaction occurred in an analyte concentration-dependent manner. In the association phase (0−120 s), the intensity of SPR increased, indicating that oxidized human GapDH bound to the full-length and mini TrpRS specifically, and in the dissociation phase (120−360 s), the intensity of SPR decreased, indicating that oxidized human GapDH dissociated from the immobilized full-length and mini TrpRS. Binding parameters for the interaction of oxidized GapDH with full-length and mini TrpRS were determined: association rate constant $k_a = 2.3 \times 10^3$ and 3.5×10^3 M^{-1} s^{-1}, dissociation rate constant $k_d = 2.2 \times 10^{-3}$ and 2.8×10^{-3} s^{-1}, and equilibrium dissociation constant K_d ($=k_d/k_a$) = 1.0 and 0.8 μM, respectively. In contrast, reduced human GapDH did not bind significantly to either full-length or mini TrpRS compared with the oxidized form (Figure 1A,B). No significant resonance signals were obtained from sensor chip surfaces without attached ligands or with BSA, indicating the absence of nonspecific interactions between the sensor chip surfaces and GapDH (data not shown).

Influence of GapDH on TrpRS Aminoacylation Activity. Aminoacyl-tRNA synthetases catalyze the first step of protein synthesis that consists of the aminoacylation of tRNAs. Since previous data showed that human TrpRS can aminoacylate yeast $tRNA^{Trp}$ *in vitro* and *in vivo* (*29*), at first we investigated aminoacylation activities of human TrpRSs toward yeast $tRNA^{Trp}$ in the absence or presence of GapDH. Reduced or oxidized human GapDH did not influence aminoacylation activities of full-length TrpRS (Figure 2). In contrast, oxidized, but not reduced, GapDH stimulated the aminoacylation activities of human mini TrpRS (Figure 2). Kinetic analyses of this aminoacylation were carried out at different concentrations of oxidized GapDH in an effort to understand how oxidized GapDH enhances TrpRS activity. Full-length TrpRS activity was not affected by the addition of oxidized GapDH (Figure 3A), suggesting that the ability

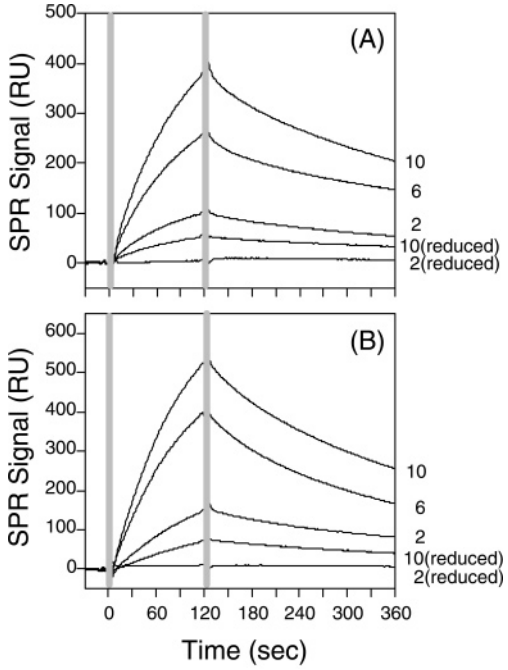

FIGURE 1: SPR analyses of oxidized and reduced GapDHs binding to human full-length or mini TrpRS. (A) Concentration dependence of oxidized and reduced forms of human GapDH on their binding affinity for human full-length TrpRS. Human full-length TrpRS was immobilized to a CM5 sensor chip. The immobilization level of human full-length TrpRS was 4200 RU. The on and off processes for ligand binding were recorded on a BIAcore instrument. The bars at 0 and 120 s indicate the start of ligand injection (association phase) and the start of injection of buffer alone (dissociation phase), respectively. Concentrations of oxidized GapDH were 2, 6, and 10 μM. The concentrations of reduced GapDH were 2 and 10 μM. (B) Concentration dependence of oxidized and reduced GapDHs on their binding affinity for human mini TrpRS. The immobilization level of human mini TrpRS was 6300 RU. Experimental conditions were the same as for panel A.

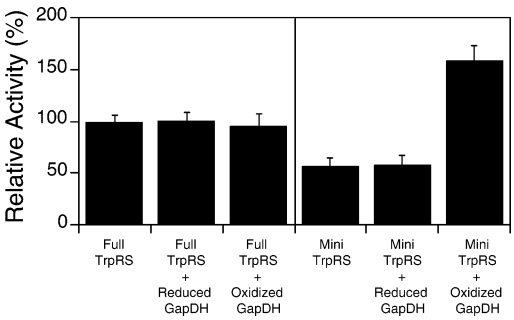

FIGURE 2: Aminoacylation activity of human full-length and mini TrpRSs toward yeast $tRNA^{Trp}$ in the absence or presence of oxidized or reduced GapDH. TrpRS (50 nM), GapDH (300 nM), and yeast tRNA (500 μM) were used. The activities of the full-length TrpRS in the absence of GapDH were normalized to 100%, and other activities were compared accordingly. Values represent the mean ± standard deviation from five experiments.

of oxidized GapDH to enhance TrpRS activity was specific to mini TrpRS. As shown in Figure 3B, oxidized GapDH significantly stimulates the catalytic activity of mini TrpRS by reducing the K_m for $tRNA^{Trp}$ 5-fold, whereas the k_{cat} value remained unchanged. To further characterize the interactions among human TrpRS, GapDH, and $tRNA^{Trp}$, we used assays to examine the aminoacylation using human $tRNA^{Trp}$. We observed almost the same results as those reported above for yeast $tRNA^{Trp}$ (data not shown).

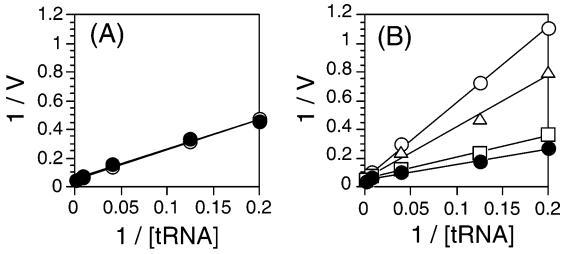

FIGURE 3: Kinetic analyses of aminoacylation activities of human TrpRSs toward yeast $tRNA^{Trp}$. (A) Analysis of the full-length TrpRS aminoacylation reaction in the absence (○) or presence of 5 μM oxidized human GapDH (●). The effect of oxidized human GapDH on the reaction was analyzed by a Lineweaver−Burk plot. TrpRS was used at a concentration of 50 nM. Total yeast tRNA was added to the reaction mixture at concentrations ranging from 5 to 500 μM (5, 8, 25, 125, and 500 μM). (B) Analysis of the mini TrpRS aminoacylation reaction at different concentrations of oxidized human GapDH. The effect of oxidized human GapDH on the reaction was analyzed by a Lineweaver−Burk plot. TrpRS (50 nM) and 0 nM (○), 50 nM (△), 500 nM (□), or 5 μM (●) oxidized GapDH were used. Total yeast tRNA was added to the reaction mixture at concentrations ranging from 5 to 500 μM (5, 8, 25, 125, and 500 μM).

Analysis of Interaction among TrpRS, GapDH, and $tRNA^{Trp}$ by Characterizing a Chimeric Protein. Human GapDH can be divided into several compact structural units called "modules", which correspond to peptides encoded by exons (*30*−*34*). Our previous experiments showed that modules are structural and functional units that are advantageous in producing stable functional proteins through the mechanism of exon shuffling (*35*−*38*). The NAD^+-binding modules consisting of 148 amino acids (Rossmann fold) of human GapDH have been reported to play important roles in binding AU-rich RNA (*39*). While at first we prepared a truncated GapDH which consisted of NH_2-terminal Rossmann fold modules (amino acids 1−150) alone, the truncated GapDH that was produced was very unstable. Since previous experiments suggest that the NH_2-terminal Rossmann fold modules interact tightly with the COOH-terminal α-helical module (Figure 4) (*40*) and that the packing among modules is quite essential for stabilization of protein conformation (*41*, *42*), we next tried to fuse the NH_2-terminal Rossmann fold modules (amino acids 1−148) of GapDH to the stable α-helical-rich protein "myoglobin (Mb)" which we designated as "modules(GapDH)-fused Mb" (Figure 4). Modules(GapDH)-fused Mb was expressed in *E. coli* and purified, and its molecular size (expected molecular size of 34 kDa) and its purity were confirmed by 12.5% SDS−polyacrylamide gel (Figure 5). Titration of modules(GapDH)-fused Mb with ferric hemin showed that the heme bound to the modules(GapDH)-fused Mb in a stoichiometric heme:protein 1:1 ratio (data not shown). The visible absorption spectra of deoxy forms of the modules(GapDH)-fused Mb and wild-type Mb exhibited a strong Soret band at 433 nm and a weak Q-band at 557 and 556 nm, respectively. In the spectrum of the CO-bound form of modules(GapDH)-fused Mb, a Soret band at 422 nm and Q-bands at 540 and 577 nm were observed, corresponding to those of wild-type Mb

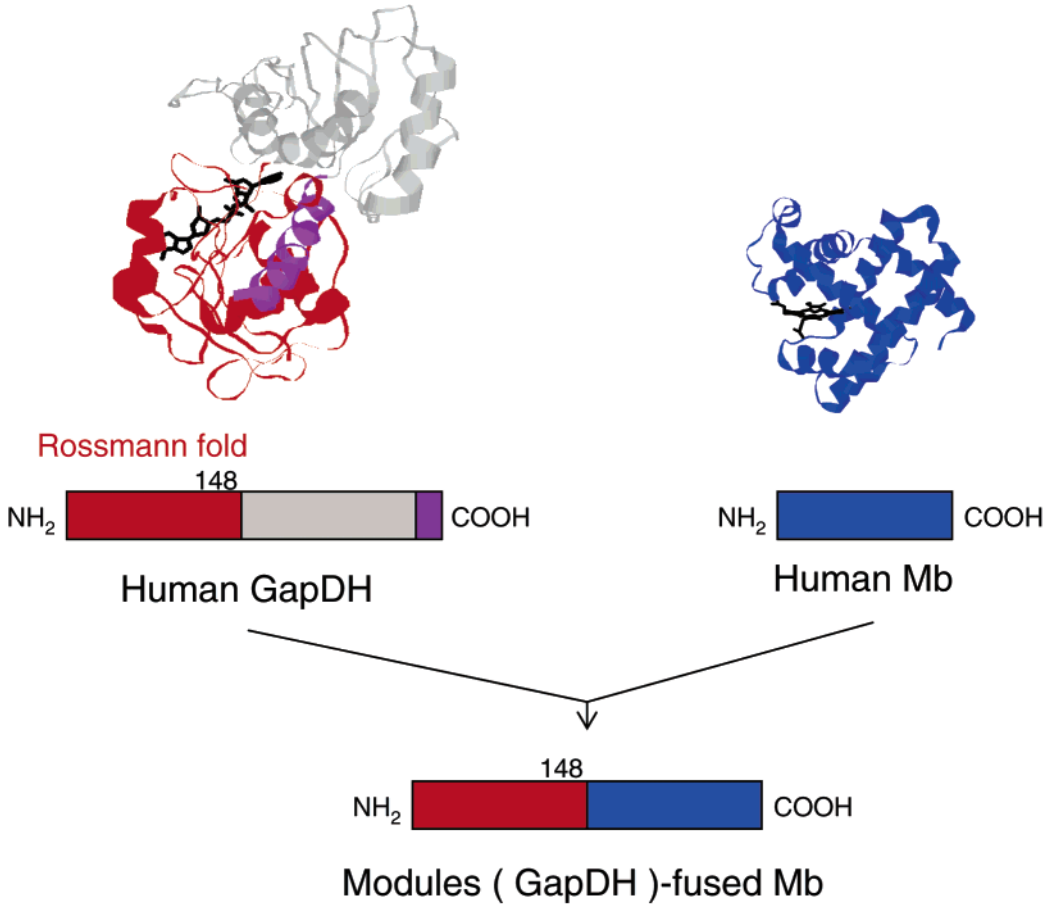

FIGURE 4: Schematic representation of the preparation of modules(GapDH)-fused Mb. Human GapDH consists of NH_2-terminal Rossmann fold modules, catalytic modules, and a COOH-terminal α-helical module. NH_2-terminal Rossmann fold modules of human GapDH (amino acids 1−148) were fused to the N-terminus of human Mb to prepare modules(GapDH)-fused Mb. NAD and heme are depicted in black.

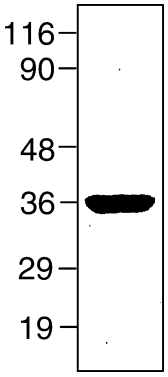

FIGURE 5: SDS−PAGE analysis of modules(GapDH)-fused Mb. The sample was analyzed on a 12.5% SDS−polyacrylamide gel and stained with Coomassie Blue. Molecular size markers are shown at the left (in kilodaltons).

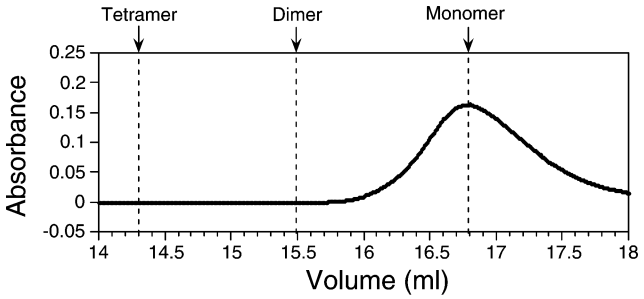

FIGURE 6: Gel filtration chromatography of modules(GapDH)-fused Mb on a Superdex 200 column of the FPLC system. The optical density profiles were monitored at 280 nm. Elution volumes of blue dextran, thyroglobulin (669 kDa), immunoglobulin G (160 kDa), BSA (67 kDa), Ngb (17 kDa), and cytochrome *c* (12 kDa) were 10.3, 11.1, 14.0, 15.6, 18.2, and 19.2 mL, respectively, and these data were used for column calibration. Expected elution volumes corresponding to the monomer (34 kDa), dimer (68 kDa), and tetramer (136 kDa) of the modules(GapDH)-fused Mb are shown.

(423, 540, and 577 nm, respectively). These data demonstrated that the modules(GapDH)-fused Mb had a Mb-like heme environmental structure.

The association property of the modules(GapDH)-fused Mb was examined by gel filtration over a calibrated FPLC Superdex 200 column. As shown in Figure 6, the modules(GapDH)-fused Mb eluted at fractions corresponding to the monomer (34 kDa). As shown in Figure 7, SPR experiments revealed that the modules(GapDH)-fused Mb, but not wild-type Mb, interacted with mini TrpRS, suggesting that TrpRS binds to the NH_2-terminal Rossmann fold region of GapDH. Binding parameters for the interaction of modules(GapDH)-fused Mb with full-length and mini TrpRS were determined: association rate constant $k_a = 5.4 \times 10^3$ and 8.0×10^3 M^{-1} s^{-1}, dissociation rate constant $k_d = 7.1 \times 10^{-3}$ and 4.0×10^{-3} s^{-1}, and equilibrium dissociation constant $K_d = k_d/k_a = 1.3$ and 0.5 μM, respectively. We then investigated the aminoacylation ability of the modules(GapDH)-fused Mb. As shown in Figure 8, the aminoacylation assay results showed that the modules(GapDH)-fused Mb stimulated the aminoacylation of mini TrpRS as did human GapDH. As a control, we found that wild-type Mb did not have any effects on the aminoacylation of mini TrpRS (Figure 8). These data suggest that the NH_2-terminal Rossmann fold region of GapDH is crucial for its ability to interact with mini TrpRS as well as tRNA and for the regulation of its aminoacylation of mini TrpRS.

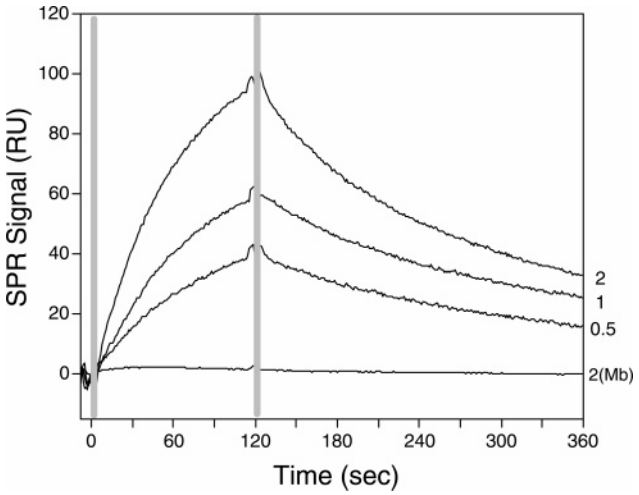

FIGURE 7: SPR analyses of modules(GapDH)-fused Mb and wild-type Mb binding to human mini TrpRS. The immobilization level of human mini TrpRS was 6300 RU. The concentrations of the modules(GapDH)-fused Mb were 0.5, 1, and 2 μM, while the concentration of wild-type Mb was 2 μM.

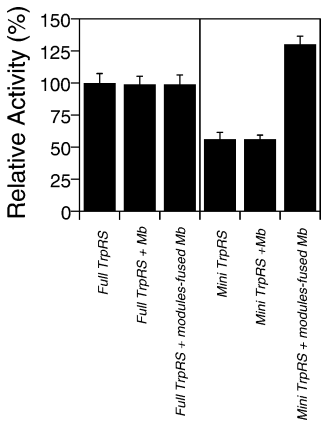

FIGURE 8: Aminoacylation activity of human full-length and mini TrpRSs toward yeast $tRNA^{Trp}$ in the absence or presence of modules(GapDH)-fused Mb or wild-type Mb. Concentrations were 50 nM TrpRS, 300 nM modules(GapDH)-fused Mb or wild-type Mb, and 500 μM yeast tRNA. The activities of full-length TrpRS alone were normalized to 100%, and other activities were compared accordingly. Values represent the mean ± standard deviation from five experiments.

DISCUSSION

In this study, we demonstrated that an oxidized, but not reduced, form of human GapDH interacts with both full-length and mini TrpRSs and specifically increases the aminoacylation activity of mini, but not full-length, TrpRS. Specific stimulation of mini TrpRS aminoacylation activity by oxidized GapDH is noteworthy since this effect may be associated with its ability to act as an angiostatic factor. This is the first example of modulation of aminoacylation activity by oxidative stress. We recently reported that human neuroglobin (Ngb) was an oxidative stress-responsive sensor (*43*−*45*). Specifically, human Ngb can function as a guanine nucleotide dissociation inhibitor for the α-subunit of heterotrimeric G protein during oxidative-stress conditions (*43*). While oxidation of human Ngb induces large tertiary structural changes around heme due to the ligation of distal histidine to heme iron (*43*), human GapDH induces post-translational modifications of a Cys residue during oxidative stress (*20*−*24*).

Effects of GapDH Cys Modification by Oxidative Stress. GapDH is a target of oxidative stress (*19*). In the presence of a low hydrogen peroxide concentration that can be generated under oxidative-stress conditions, an essential Cys of human GapDH is oxidized to its sulfenate derivative (*21*). It has been reported that the oxidation of SH groups in the active site of GapDH strongly enhanced its binding to tRNA (*26*). Since tRNA induces the dissociation of GapDH tetramers into monomers or dimers (*26*, *46*, *47*), oxidized GapDH could easily dissociate into a monomer or dimer.

In this study, we engineered a model of monomeric GapDH Rossmann fold modules(GapDH)-fused Mb and demonstrated that it bound to mini TrpRS and stimulated the aminoacylation activity of mini TrpRS. Moreover, our results clarified that the NH_2-terminal Rossmann fold region of GapDH is crucial for its binding to mini TrpRS as well as tRNA and for the regulation of the aminoacylation activity of mini TrpRS. The modules(GapDH)-fused Mb does not contain the essential Cys of human GapDH. These results suggest that the GapDH Cys modification may expose the Rossmann fold in GapDH.

The oxidized, but not reduced, form of GapDH binds to mini TrpRS and can stimulate its aminoacylation activity. Recently, another report concerning the regulation of protein−protein interactions by the hydrogen peroxide-dependent modification of GapDH has been published (*48*): modification of GapDH on Cys by hydrogen peroxide endows GapDH with the ability to bind phospholipase D2 (PLD2), and the resulting association is involved in the regulation of PLD2 activity by hydrogen peroxide (*48*). These results suggest that the oxidation of GapDH induces a conformational change in the enzyme that triggers changes in its affinity for binding to its molecular targets. Thus, GapDH might act as a sensor to transmit the signaling of oxidative stress.

Regulation of Aminoacylation Efficiency by Cis- and Trans-Acting Factors. Aminoacyl-tRNA synthetases have adopted nonconserved RNA binding domains in *cis* or in *trans* to enhance their catalytic efficiency or substrate specificity (*4*−*7*, *49*−*54*). Although the C-terminal extension of plant methionyl-tRNA synthetase is a case of the *cis*-acting domain, yeast Arc1p and mammalian EMAP II are examples of *trans*-acting factors (*50*, *52*−*54*).

In this study, the K_m (tRNA) value of full-length TrpRS was found to be 2-fold lower than that of mini TrpRS, indicating that full-length TrpRS binds to $tRNA^{Trp}$ more tightly than mini TrpRS. This feature could be a means by which the local concentration of tRNA could be increased to improve the efficacy of the protein translation machinery in eukaryotic cells. Because the free tRNA concentration is nonsaturating within the cell, we can conclude that the NH_2-terminally appended domain of full-length TrpRS acts as a *cis*-acting cofactor for aminoacylation. The aminoacylation activity of mini TrpRS was enhanced approximately 5-fold by its interaction with oxidized, but not reduced, GapDH. In contrast, no change in catalytic efficiency was observed for full-length TrpRS. While the function of full-length TrpRS was exerted by the NH_2-terminal peptide extension connected in *cis* to the catalytic domain of TrpRS, in the case of mini TrpRS, oxidized GapDH acted as a *trans*-acting cofactor for aminoacylation. The tRNA binding capability of the Rossmann fold will be critical for the role of oxidized GapDH. This *trans*-acting factor may be more functionally flexible than the *cis*-acting peptide extension because it can easily dissociate from TrpRS and interact with cellular molecules that are involved in other physiological processes.

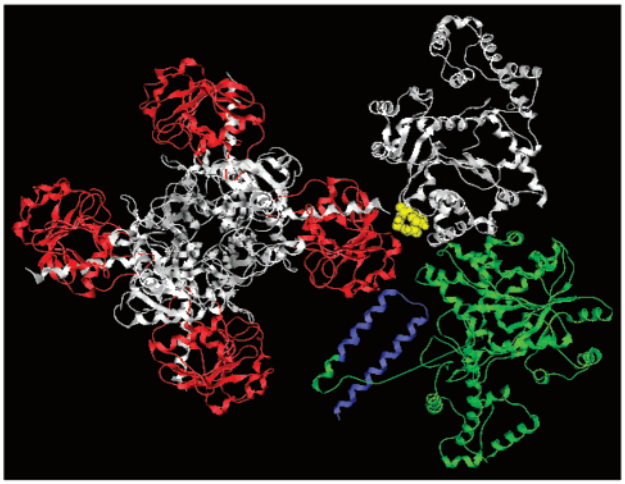

FIGURE 9: Putative binding of dimeric human full-length TrpRS to tetrameric GapDH. Only one monomer of TrpRS is colored and consists of the NH_2-terminally appended domain (blue) and the catalytic domain (green). In the other monomer (gray), the first 96 residues, including the NH_2-terminally appended domain, are disordered and the residues corresponding to the insertion sites of the extra peptide in *A. ferrooxidans* TrpRS are colored yellow. Human GapDH is a homotetramer, in which each monomer consists of the NH_2-terminal Rossmann fold modules (red) and other modules (gray).

Possible Binding Site in Human TrpRS for Oxidized GapDH. Acidithiobacillus ferrooxidans TrpRS contains a peptide insert of 70 amino acids in its catalytic domain (*55*). Zúñiga et al. used BLAST to search protein sequence databases for this peptide sequence and pointed out that its sequence is similar to a portion of the Rossmann fold of certain dehydrogenases (*55*). It should be also noted that the deletion of this peptide sequence from *A. ferrooxidans* TrpRS caused a 7-fold increase in the K_m for $tRNA^{Trp}$, as compared with that of wild-type TrpRS, although the k_{cat} value remained unchanged (*55*), suggesting that this peptide insertion in *A. ferrooxidans* TrpRS acts as a *cis*-acting factor.

On the basis of the insertion site of the peptide in *A. ferrooxidans* TrpRS, we predicted a possible binding site in human TrpRS for oxidized GapDH. As shown in Figure 9, the binding site of GapDH is predicted to be located near the NH_2-terminally appended domain of human full-length TrpRS. This is consistent with a previous study showing that a monoclonal antibody against this NH_2-terminal domain of human full-length TrpRS strongly interferes with the binding of full-length TrpRS to GapDH (*18*).

In this study, we have shown that human oxidized GapDH interacts with both full-length and mini TrpRSs and specifically increases the aminoacylation activity of mini, but not full-length, TrpRS. Why does oxidized GapDH not activate full-length TrpRS, even though it has similar binding affinities for both TrpRSs? We speculate that when full-length TrpRS binds to $tRNA^{Trp}$, conformational changes in the protein may lead to the dissociation of GapDH because of steric hindrance between GapDH and the NH_2-terminally appended domain of full-length TrpRS.

Possible Intracellular Roles of Human Mini TrpRS. Human TrpRS was reported to be upregulated during the maturation

of human monocytes to macrophages (*56*). Moreover, TrpRS expression was found to be upregulated during maturation of immature dendritic cells from peripheral blood monocytes and appeared to be a good marker of the final stage of maturation and differentiation of monocyte-derived dendritic cells (*57*). Both macrophages and dendritic cells are known to be antigen-presenting cells. Immune system proteins that mediate immune activation, e.g., human major histocompatibility complex (MHC) class I and class II, β_2-microglobulin, and complement factor B, are all induced by IFN and are all exceptionally enriched in Trp residues, as compared to human proteins in general (*58*−*60*). By using immunoelectron microscopy, Paley et al. found that mammalian TrpRS is located on polyribosomes bound to rough endoplasmic reticulum membranes and, moreover, clarified that a 50 kDa fragment (corresponding to mini TrpRS), but not full-length TrpRS, exists in a Triton-insoluble fraction that includes the endoplasmic reticulum (*61*). It should also be noted that oxidative stress induces the maturation of human dendritic cells (*62*) and that reactive oxygen species are produced under the oxidative-stress conditions that occur during phagocytosis (*24*). Therefore, association of human mini TrpRS with oxidized GapDH may help in safeguarding Trp incorporation of synthesis of immunological molecules, e.g., MHC molecules, on rough endoplasmic reticulum in antigen-presenting cells. Studies are now in progress to elucidate the physiological significance of the stimulation of aminoacylation activity of mini TrpRS by oxidized GapDH under conditions of oxidative stress. Further studies will be required to clarify the involvement of mini TrpRS in the regulation of both translation and angiogenesis.

REFERENCES

1. Garret, M., Pajot, B., Trézéguet, V., Labouesse, J., Merle, M., Gandar, J.-C., Benedetto, J.-P., Sallafranque, M.-L., Alterio, J., Gueguen, M., Sarger, C., Labouesse, B., and Bonnet, J. (1991) A mammalian tryptophanyl-tRNA synthetase shows little homology to prokaryotic synthetases but near identity with mammalian peptide chain release factor, *Biochemistry 30*, 7809−7817.
2. Frolova, L. Y., Grigorieva, A. Y., Sudomoina, M. A., and Kisselev, L. L. (1993) The human gene encoding tryptophanyl-tRNA synthetase: Interferon-response elements and exon-intron organization, *Gene 128*, 237−245.
3. Shiba, K. (2002) Intron positions delineate the evolutionary path of a pervasively appended peptide in five human aminoacyl-tRNA synthetases, *J. Mol. Evol. 55*, 727−733.
4. Raben, N., Nichols, R., Dohlman, J., McPhie, P., Sridhar, V., Hyde, C., Leff, R., and Plotz, P. (1994) A motif in human histidyl-tRNA synthetase which is shared among several aminoacyl-tRNA synthetases is a coiled-coil that is essential for enzymatic activity and contains the major autoantigenic epitope, *J. Biol. Chem. 269*, 24277−24283.
5. Cahuzac, B., Berthonneau, E., Birlirakis, N., Guittet, E., and Mirande, M. (2000) A recurrent RNA-binding domain is appended to eukaryotic aminoacyl-tRNA synthetases, *EMBO J. 19*, 445−452.
6. Jeong, E.-J., Hwang, G.-S., Kim, K. H., Kim, M. J., Kim, S., and Kim, K.-S. (2000) Structural analysis of multifunctional peptide motifs in human bifunctional tRNA synthetase: Identification of RNA-binding residues and functional implications for tandem repeats, *Biochemistry 39*, 15775−15782.
7. Kaminska, M., Shalak, V., and Mirande, M. (2001) The appended C-domain of human methionyl-tRNA synthetase has a tRNA-sequestering function, *Biochemistry 40*, 14309−14316.
8. Yang, X.-L., Otero, F. J., Skene, R. J., McRee, D. E., Schimmel, P., and Ribas de Pouplana, L. (2003) Crystal structures that suggest late development of genetic code components for differentiating aromatic side chains, *Proc. Natl. Acad. Sci. U.S.A. 100*, 15376−15380.
9. Kise, Y., Lee, S. W., Park, S. G., Fukai, S., Sengoku, T., Ishii, R., Yokoyama, S., Kim, S., and Nureki, O. (2004) A short peptide insertion crucial for angiostatic activity of human tryptophanyl-tRNA synthetase, *Nat. Struct. Mol. Biol. 11*, 149−156.
10. Yu, Y., Liu, Y., Shen, N., Xu, X., Xu, F., Jia, J., Jin, Y., Arnold, E., and Ding, J. (2004) Crystal structure of human tryptophanyl-tRNA synthetase catalytic fragment: Insights into substrate recognition, tRNA binding, and angiogenesis activity, *J. Biol. Chem. 279*, 8378−8388.
11. Yang, X.-L., Schimmel, P., and Ewalt, K. L. (2004) Relationship of two human tRNA synthetases used in cell signaling, *Trends Biochem. Sci. 29*, 250−256.
12. Tolstrup, A. B., Bejder, A., Fleckner, J., and Justesen, J. (1995) Transcriptional regulation of the interferon-γ-inducible tryptophanyl-tRNA synthetase includes alternative splicing, *J. Biol. Chem. 270*, 397−403.
13. Turpaev, K. T., Zakhariev, V. M., Sokolova, I. V., Narovlyansky, A. N., Amchenkova, A. M., Justesen, J., and Frolova, L. Y. (1996) Alternative processing of the tryptophanyl-tRNA synthetase mRNA from interferon-treated human cells, *Eur. J. Biochem. 240*, 732−737.
14. Shaw, A. C., Larsen, M. R., Roepstorff, P., Justesen, J., Christiansen, G., and Birkelund, S. (1999) Mapping and identification of interferon γ-regulated HeLa cell proteins separated by immobilized pH gradient two-dimensional gel electrophoresis, *Electrophoresis 20*, 984−993.
15. Kisselev, L., Frolova, L., and Haenni, A.-L. (1993) Interferon inducibility of mammalian tryptophanyl-tRNA synthetase: New perspectives, *Trends Biochem. Sci. 18*, 263−267.
16. Fleckner, J., Martensen, P. M., Tolstrup, A. B., Kjeldgaard, N. O., and Justesen, J. (1995) Differential regulation of the human, interferon inducible tryptophanyl-tRNA synthetase by various cytokines in cell lines, *Cytokine 7*, 70−77.
17. Wakasugi, K., Slike, B. M., Hood, J., Otani, A., Ewalt, K. L., Friedlander, M., Cheresh, D. A., and Schimmel, P. (2002) A human aminoacyl-tRNA synthetase as a regulator of angiogenesis, *Proc. Natl. Acad. Sci. U.S.A. 99*, 173−177.
18. Filonenko, V. V., Beresten, S. F., Rubikaite, B. I., and Kisselev, L. L. (1989) Bovine tryptophanyl-tRNA synthetase and glyceraldehyde-3-phosphate dehydrogenase from a complex, *Biochem. Biophys. Res. Commun. 161*, 481−488.
19. Eaton, P., Byers, H. L., Leeds, N., Ward, M. A., and Shattock, M. J. (2002) Detection, quantitation, purification, and identification of cardiac proteins S-thiolated during ischemia and reperfusion, *J. Biol. Chem. 277*, 9806−9811.
20. Little, C., and O'Brien, P. J. (1969) Mechanism of peroxide-inactivation of the sulphydryl enzyme glyceraldehyde-3-phosphate dehydrogenase, *Eur. J. Biochem. 10*, 533−538.
21. Schmalhausen, E. V., Nagradova, N. K., Boschi-Muller, S., Branlant, G., and Muronetz, V. I. (1999) Mildly oxidized GAPDH: The coupling of the dehydrogenase and acyl phosphatase activities, *FEBS Lett. 452*, 219−222.
22. Molina y Vedia, L., McDonald, B., Reep, B., Brüne, B., Di Silvio, M., Billiar, T. R., and Lapetina, E. G. (1992) Nitric oxide-induced *S*-nitrosylation of glyceraldehyde-3-phosphate dehydrogenase inhibits enzymatic activity and increases endogenous ADP-ribosylation, *J. Biol. Chem. 267*, 24929−24932.
23. Mohr, S., Hallak, H., de Boitte, A., Lapetina, E. G., and Brüne, B. (1999) Nitric oxide-induced *S*-glutathionylation and inactivation of glyceraldehyde-3-phosphate dehydrogenase, *J. Biol. Chem. 274*, 9427−9430.
24. Ravichandran, V., Seres, T., Moriguchi, T., Thomas, J. A., and Johnston, R. B., Jr. (1994) *S*-Thiolation of glyceraldehyde-3-phosphate dehydrogenase induced by the phagocytosis-associated respiratory burst in blood monocytes, *J. Biol. Chem. 269*, 25010−25015.
25. Singh, R., and Green, M. R. (1993) Sequence-specific binding of transfer RNA by glyceraldehyde-3-phosphate dehydrogenase, *Science 259*, 365−368.
26. Arutyunova, E. I., Danshina, P. V., Domnina, L. V., Pleten, A. P., and Muronetz, V. I. (2003) Oxidation of glyceraldehyde-3-phosphate dehydrogenase enhances its binding to nucleic acids, *Biochem. Biophys. Res. Commun. 307*, 547−552.
27. Varadarajan, R., Lambright, D. G., and Boxer, S. G. (1989) Electrostatic interactions in wild-type and mutant recombinant human myoglobins, *Biochemistry 28*, 3771−3781.

28. Kisselev, L. L., Favorova, O. O., Nurbekov, M. K., Dmitriyenko, S. G., and Engelhardt, W. A. (1981) Bovine tryptophanyl-tRNA synthetase. A zinc metalloenzyme, *Eur. J. Biochem. 120*, 511−517.
29. Johnson, J. D., Spellmann, J. M., White, K. H., Barr, K. K., and John, T. R. (2002) Human tryptophanyl-tRNA synthetase can efficiently complement the *Saccharomyces cerevisiae* homologue, Wrs1P, *FEMS Microbiol. Lett. 216*, 111−115.
30. Go, M. (1981) Correlation of DNA exonic regions with protein structural units in haemoglobin, *Nature 291*, 90−92.
31. Go, M. (1983) Modular structural units, exons, and function in chicken lysozyme, *Proc. Natl. Acad. Sci. U.S.A. 80*, 1964−1968.
32. Ercolani, L., Florence, B., Denaro, M., and Alexander, M. (1988) Isolation and complete sequence of a functional human glyceraldehyde-3-phosphate dehydrogenase gene, *J. Biol. Chem. 263*, 15335−15341.
33. Kersanach, R., Brinkmann, H., Liaud, M.-F., Zhang, D.-X., Martin, W., and Cerff, R. (1994) Five identical intron positions in ancient duplicated genes of eubacterial origin, *Nature 367*, 387−389.
34. Long, M., De Souza, S. J., Rosenberg, C., and Gilbert, W. (1996) Exon shuffling and the origin of the mitochondrial targeting function in plant cytochrome *c*1 precursor, *Proc. Natl. Acad. Sci. U.S.A. 93*, 7727−7731.
35. Gilbert, W. (1978) Why genes in pieces? *Nature 271*, 501.
36. Blake, C. C. (1979) Exons encode protein functional units, *Nature 277*, 598.
37. Wakasugi, K., Ishimori, K., Imai, K., Wada, Y., and Morishima, I. (1994) "Module" substitution in hemoglobin subunits: Preparation and characterization of a "chimera $\beta\alpha$-subunit", *J. Biol. Chem. 269*, 18750−18756.
38. Wakasugi, K., Quinn, C. L., Tao, N., and Schimmel, P. (1998) Genetic code in evolution: Switching species-specific aminoacylation with a peptide transplant, *EMBO J. 17*, 297−305.
39. Nagy, E., and Rigby, W. F. C. (1995) Glyceraldehyde-3-phosphate dehydrogenase selectively binds AU-rich RNA in the NAD^+-binding region (Rossmann fold), *J. Biol. Chem. 270*, 2755−2763.
40. Mercer, W. D., Winn, S. I., and Watson, H. C. (1976) Twinning in crystals of human skeletal muscle D-glyceraldehyde-3-phosphate dehydrogenase, *J. Mol. Biol. 104*, 277−283.
41. Biro, J., Fabry, S., Dietmaier, W., Bogedain, C., and Hensel, R. (1990) Engineering thermostability in archaebacterial glyceraldehyde-3-phosphate dehydrogenase. Hints for the important role of interdomain contacts in stabilizing protein conformation, *FEBS Lett. 275*, 130−134.
42. Wakasugi, K., Ishimori, K., and Morishima, I. (1997) "Module"-substituted globins: Artificial exon shuffling among myoglobin, hemoglobin α- and β-subunits, *Biophys. Chem. 68*, 265−273.
43. Wakasugi, K., Nakano, T., and Morishima, I. (2003) Oxidized human neuroglobin as a heterotrimeric Gα protein guanine nucleotide dissociation inhibitor, *J. Biol. Chem. 278*, 36505−36512.
44. Wakasugi, K., Nakano, T., Kitatsuji, C., and Morishima, I. (2004) Human neuroglobin interacts with flotillin-1, a lipid raft microdomain-associated protein, *Biochem. Biophys. Res. Commun. 318*, 453−460.
45. Wakasugi, K., Nakano, T., and Morishima, I. (2004) Association of human neuroglobin with cystatin C, a cysteine proteinase inhibitor, *Biochemistry 43*, 5119−5125.
46. Ovádi, J., Telegdi, M., Batke, J., and Keleti, T. (1971) Functional non-identity of subunits and isolation of active dimers of D-glyceraldehyde-3-phosphate dehydrogenase, *Eur. J. Biochem. 22*, 430−438.
47. Nagy, E., Henics, T., Eckert, M., Miseta, A., Lightowlers, R. N., and Kellermayer, M. (2000) Identification of the NAD^+-binding fold of glyceraldehyde-3-phosphate dehydrogenase as a novel RNA-binding domain, *Biochem. Biophys. Res. Commun. 275*, 253−260.
48. Kim, J. H., Lee, S., Park, J. B., Lee, S. D., Kim, J. H., Ha, S. H., Hasumi, K., Endo, A., Suh, P.-G., and Ryu, S. H. (2003) Hydrogen peroxide induces association between glyceraldehyde 3-phosphate dehydrogenase and phospholipase D2 to facilitate phospholipase D2 in PC12 cells, *J. Neurochem. 85*, 1228−1236.
49. Chihade, J. W., and Schimmel, P. (1999) Assembly of a catalytic unit for RNA microhelix aminoacylation using nonspecific RNA binding domains, *Proc. Natl. Acad. Sci. U.S.A. 96*, 12316−12321.
50. Kaminska, M., Deniziak, M., Kerjan, P., Barciszewski, J., and Mirande, M. (2000) A recurrent general RNA binding domain appended to plant methionyl-tRNA synthetase acts as a *cis*-acting cofactor for aminoacylation, *EMBO J. 19*, 6908−6917.
51. Wang, C.-C., and Schimmel, P. (1999) Species barrier to RNA recognition overcome with nonspecific RNA binding domains, *J. Biol. Chem. 274*, 16508−16512.
52. Simos, G., Sauer, A., Fasiolo, F., and Hurt, E. C. (1998) A conserved domain with Arc1p delivers tRNA to aminoacyl-tRNA synthetases, *Mol. Cell 1*, 235−242.
53. Park, S. G., Jung, K. H., Lee, J. S., Jo, Y. J., Motegi, H., Kim, S., and Shiba, K. (1999) Precursor of pro-apoptotic cytokine modulates aminoacylation activity of tRNA synthetase, *J. Biol. Chem. 274*, 16673−16676.
54. Deinert, K., Fasiolo, F., Hurt, E. C., and Simos, G. (2001) Arc1p organizes the yeast aminoacyl-tRNA synthetase complex and stabilizes its interaction with the cognate tRNAs, *J. Biol. Chem. 276*, 6000−6008.
55. Zúñiga, R., Salazar, J., Canales, M., and Orellana, O. (2002) A dispensable peptide from *Acidithiobacillus ferrooxidans* tryptophanyl-tRNA synthetase affects tRNA binding, *FEBS Lett. 532*, 387−390.
56. Krause, S. W., Rehli, M., Kreutz, M., Schwarzfischer, L., Paulauskis, J. D., and Andreesen, R. (1996) Differential screening identifies genetic markers of monocyte to macrophage maturation, *J. Leukocyte Biol. 60*, 540−545.
57. Matsunaga, T., Ishida, T., Takekawa, M., Nishimura, S., Adachi, M., and Imai, K. (2002) Analysis of gene expression during maturation of immature dendritic cells derived from peripheral blood monocytes, *Scand. J. Immunol. 56*, 593−601.
58. Xue, H., and Wong, J. T.-F. (1995) Interferon induction of human tryptophanyl-tRNA synthetase safeguards the synthesis of tryptophan-rich immune-system proteins: A hypothesis, *Gene 165*, 335−339.
59. Boehm, U., Klamp, T., Groot, M., and Howard, J. C. (1997) Cellular responses to interferon-γ, *Annu. Rev. Immunol. 15*, 749−795.
60. Schroder, K., Hertzog, P. J., Ravasi, T., and Hume, D. A. (2004) Interferon-γ: An overview of signals, mechanisms and functions, *J. Leukocyte Biol. 75*, 163−189.
61. Paley, E. L., Baranov, V. N., Alexandrova, N. M., and Kisselev, L. L. (1991) Tryptophanyl-tRNA synthetase in cell lines resistant to tryptophan analogs, *Exp. Cell Res. 195*, 66−78.
62. Kantengwa, S., Jornot, L., Devenoges, C., and Nicod, L. P. (2003) Superoxide anions induce the maturation of human dendritic cells, *Am. J. Crit. Care Med. 167*, 431−437.

BI048313K